

CMoE: Converting Mixture-of-Experts from Dense to Accelerate LLM Inference

Zehua Pei¹, Lancheng Zou¹, Hui-Ling Zhen², Xianzhi Yu², Wulong Liu²,
Sinno Jialin Pan¹, Mingxuan Yuan², Bei Yu¹

¹The Chinese University of Hong Kong

²Noah’s Ark Lab, Huawei

Abstract

Scaling large language models (LLMs) improves performance but dramatically increases inference costs. The feed-forward network (FFN), consuming approximately 70% of inference compute, represents a critical bottleneck, particularly in large batch size scenarios. While mixture-of-experts (MoE) architectures leverage activation sparsity for efficiency, converting existing dense models to MoEs traditionally requires resource-intensive continual pre-training. We present CMoE, a framework that rapidly transforms dense LLMs into MoEs without training. The key innovation lies in analyzing FFN neuron activations to partition them into shared (always active) and routed experts. Routed neurons are clustered using a balanced assignment algorithm, and a differentiable router is constructed analytically from activation statistics, enabling immediate deployment or optional lightweight fine-tuning. Experiments demonstrate that, with activation ratio of 75%, it achieves remarkable results, delivering lossless precision in terms of perplexity while still maintaining a 5% acceleration. Further experiments reveal that a CMoE configuration activating just 25% of parameters reduces end-to-end latency by 1.5× while preserving usable perplexity without additional training. Moreover, a brief LoRA fine-tuning process (requiring only 1 hour and 2,000 samples) successfully recovers over 76% of the dense model’s downstream accuracy. By effectively balancing performance and efficiency, CMoE offers a viable path forward for deploying LLMs in real-world scenarios where computational resources are limited. We make our code publicly available at <https://github.com/JarvisPei/CMoE>.

1 Introduction

Large language models (LLMs) achieve remarkable performance [1, 2, 3, 4], but their growing size presents deployment challenges due to high computational demands, especially on resource-constrained hardware or under strict latency budgets. The mixture-of-experts (MoE) architecture [5, 6, 7, 8] offers a path forward. Instead of activating all parameters per token like dense models, MoEs use sparse feed-forward networks (FFNs) composed of specialized sub-networks (experts) selected by a dynamic router. This decouples model capacity from computational cost.

In modern LLMs such as the Llama-series and DeepSeek-series, FFN blocks are responsible for approximately 70% of both inference FLOPs and memory traffic. As batch sizes increase, a common strategy for maximizing hardware utilization and throughput, models increasingly operate in a compute-bound regime, where computational power becomes the limiting factor for inference speed.

Given the FFN’s disproportionate contribution to memory and computational demands, sparsifying FFNs has become a primary target for efficiency improvement. Several studies have reported high activation sparsity in FFN neurons [9, 10, 11], inspiring a wave of techniques that aim to restructure dense FFN layers into sparse mixtures of experts (MoEs) by reorganizing existing parameters [12, 13, 14]. These MoE conversions can dramatically reduce both memory usage and computational overhead, improving throughput, particularly in large-batch, latency-sensitive inference scenarios.

Preprint.

However, despite their promise, such methods generally require substantial additional computation and large-scale datasets for continual pre-training or fine-tuning after conversion, in order to recover or maintain model quality. This retraining step can be prohibitively expensive and slow, posing a significant barrier to rapid deployment in production environments. As a result, there is growing interest in developing lightweight strategies that minimize retraining costs while delivering tangible inference speedups in real-world settings.

To overcome this bottleneck, we propose **CMoE**, a framework to efficiently *convert* dense LLMs into MoE architectures *without requiring any training*. The conversion process leverages the existing knowledge within the dense model’s FFN and completes in under five minutes on a single GPU. CMoE first analyzes neuron activation patterns across a small calibration dataset to distinguish frequently active neurons (grouped into *shared* experts) from sparsely active ones (grouped into *routed* experts). Routed experts are formed by clustering neurons using a balanced assignment algorithm [15] to maintain activation coherence. Crucially, CMoE then constructs a differentiable routing mechanism *analytically* from activation statistics, bypassing the need for router training and enabling immediate use or subsequent lightweight fine-tuning.

Our contributions are:

- **Training-free conversion.** CMoE rapidly restructures dense FFNs into shared and routed experts using activation analysis and balanced assignment, requiring only minutes and no gradient updates. In practical implementation, it is found that with an activation ratio of 75%, it achieves remarkable results, delivering lossless precision in terms of perplexity while still maintaining a 5% acceleration.
- **Analytical, differentiable router.** The router is initialized directly from activation statistics, providing immediate functionality and a strong starting point for optional fine-tuning.
- **Controllable performance-efficiency trade-off.** CMoE allows adjusting the expert activation ratio. Experiments show a spectrum from $1.5\times$ latency reduction (at 25% activation) to near-dense perplexity (at 75% activation). Minimal fine-tuning (1 hour, 2k samples) recovers $>76\%$ of dense model downstream accuracy.

CMoE’s combination of speed, flexibility, and training-free nature presents a compelling solution for researchers and practitioners requiring efficient, low-overhead deployment of LLMs.

2 Related Work

In contrast to pretraining MoE models from scratch, recent research has investigated the feasibility of constructing MoE architectures by repurposing existing dense LLMs. Current methodologies for deriving MoE models from dense checkpoints generally follow two paradigms: (1) partitioning parameters of FFNs while preserving the original model’s total parameter count [16, 10, 17], or (2) expanding the model’s overall capacity while retaining activation dimensions comparable to standard dense models [18, 19]. This work prioritizes the former approach. Notably, MoEBERT [16] introduces an importance-driven strategy to transform FFNs into expert modules by strategically redistributing top-scoring neurons across specialized components. Concurrently, MoEfication [10] leverages the discovery of sparse activation patterns in ReLU-based FFNs within T5 architectures, enabling the decomposition of these layers into distinct expert groups governed by a learned routing mechanism. Based on continual training, [12] modifies the LLaMA-2 7B model as a LLaMA-MoE-3.5B MoE model, where the parameters of the original FFNs are partitioned into multiple experts. In [13], based on a two-stage post-training strategy, an MoE model is constructed from the LLaMA3 8B model, where both attention and MLP are partitioned into MoE blocks.

Note that model compression such as pruning and quantization is another important technique for efficient LLM inference [20, 21, 22, 23, 24]. Pruning is among the most widely utilized approaches to detect and remove redundant or less significant parameters from models, thereby resulting in a sparser weight matrix and faster inference. ShortGPT [25] determines the layer-removal by the similarity between a layer’s input and output. SliceGPT [26] substitutes each weight matrix with a smaller dense matrix to decrease the embedding dimension. By taking into account contextual sparsity in real time, DeJa Vu [9] has been proposed to accelerate LLM inference. In contrast to the post-training methods, Learn-To-be-Efficient is designed to train efficiency-aware LLMs so that they learn to activate fewer neurons and achieve a more favorable trade-off between sparsity and performance.

3 Methodology

CMoE transforms dense LLMs into sparsely activated MoE architectures through two key phases: efficient expert grouping and training-free router construction, followed by optional lightweight adaptation. As shown in Figure 1(a), CMoE operates through the following systematic process:

A. Neuron Activation Profiling (Section 3.1) Using a small calibration dataset, CMoE profiles the activation patterns of neurons within each FFN layer to categorize them into shared experts (high-activation, task-agnostic) and routed experts (sparsely activated, task-specific).

B. Expert Grouping (Section 3.1) **Shared Experts:** Neurons exhibiting the highest activation rates are directly assigned to shared experts, which remain consistently activated during inference. **Routed Experts:** The remaining neurons are efficiently partitioned into routed experts through balanced clustering, mathematically formulated as a linear assignment problem.

C. Router Construction (Section 3.2) The routing mechanism is analytically derived from the activation statistics of representative neurons in each expert cluster, effectively eliminating the need for computationally expensive end-to-end training.

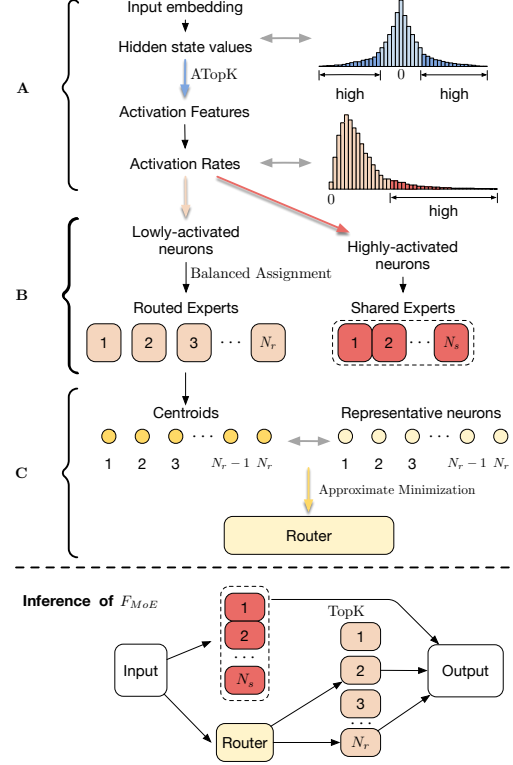


Figure 1: The overview of our proposed CMoE.

We further enhance CMoE by making the routing function differentiable (Section 3.3), facilitating further alignment and performance recovery by optional fine-tuning when resources permit.

3.1 Shared and Routed Experts Grouping

Note that an FFN exists in the tail of each transformer block, which gets the input embedding $\mathbf{x} \in \mathbb{R}^d$ and then contributes to the output together with the residual connection, i.e. $\mathbf{x} + F(\mathbf{x})$. Typically, an FFN is a two-layer fully connected network, i.e. the up projection and down projection layers, with an activation function between them. For LLaMA, the SwiGLU composes another gate projection layer. Given the up projection weight $\mathbf{W}_{up} \in \mathbb{R}^{d \times d_h}$, the gate projection weight $\mathbf{W}_{gate} \in \mathbb{R}^{d \times d_h}$ and the down projection weight $\mathbf{W}_{down} \in \mathbb{R}^{d_h \times d}$, the process of an FFN is given by:

$$F(\mathbf{x}) = \mathbf{h}\mathbf{W}_{down}, \text{ and } \mathbf{h} = \text{SwiGLU}(\mathbf{x}\mathbf{W}_{up}) = \text{Swish}(\mathbf{x}\mathbf{W}_{gate}) \odot (\mathbf{x}\mathbf{W}_{up}), \quad (1)$$

where $\text{Swish}(x) = x \cdot \sigma(x)$ is element-wise and $\sigma(\cdot)$ is the sigmoid function.

CMoE starts with grouping neurons in FFNs into experts. We construct N experts of size $m = \frac{d_h}{N}$ (assuming the intermediate size d_h is a multiple of N , i.e., $N \mid d_h$), including N_s shared experts and N_r routed experts ($N_s + N_r = N$).

Shared experts are expected to process common knowledge instead of specialization. Thus, the key idea is to group neurons that are always activated during FFN inference. Given $\mathbf{x} \in \mathbb{R}^d$ the input embedding, consider the i -th element of hidden state $\mathbf{h} \in \mathbb{R}^{d_h}$: $h_i = \text{Swish}(\mathbf{x} \cdot \mathbf{w}_{gate,i}) \cdot (\mathbf{x} \cdot \mathbf{w}_{up,i})$, where $\mathbf{w}_{gate,i} \in \mathbb{R}^d$ and $\mathbf{w}_{up,i} \in \mathbb{R}^d$ are the i -th column of $\mathbf{W}_{gate} \in \mathbb{R}^{d \times d_h}$ (gate projection weight) and $\mathbf{W}_{up} \in \mathbb{R}^{d \times d_h}$ (up projection weight), respectively. It shows that the value of h_i only depends on the input \mathbf{x} and the corresponding i -th weights, which implies the independence between neurons. On the other hand, the output of FFN can be written as:

$$F(\mathbf{x}) = \sum_{i=1}^{d_h} h_i \mathbf{w}_{down,i}, \quad (2)$$

where $\mathbf{w}_{down,i} \in \mathbb{R}^d$ is the i -th row of $\mathbf{W}_{down} \in \mathbb{R}^{d_h \times d}$ (down projection weight). When we revisit the FFN process, we can regard each h_i as the score to be multiplied to the split vector $\mathbf{w}_{down,i}$,

whose product contributes to part of the output $F(\mathbf{x})$. Therefore, we make a hypothesis:

$$\arg \min_i |h_i \mathbf{w}_{down,i}| \approx \arg \min_i |h_i|, \quad (3)$$

which is reasonable since when h_i is extremely small, the product $h_i \mathbf{w}_{down,i}$ will also vanish. In Appendix A, we conduct experiments to demonstrate that the hidden state \mathbf{h} is usually highly sparse, which means $|h_i|$ is often extremely small. Therefore, we propose a new metric, called absolute TopK (ATopK), to determine the activation status of a neuron with index i :

$$a_i = \begin{cases} 1, & |h_i| \in \text{TopK}(\{|h_j| \mid 1 \leq j \leq d_h\}, K_a), \\ 0, & \text{otherwise}, \end{cases} \quad (4)$$

where we choose neurons with K_a highest absolute value among the hidden state values, and assign their labels in the activation marker $\mathbf{a} = [a_1, a_2, \dots, a_{d_h}]$ with 1. We then obtain the set of selection indices S_{N_s} by selecting $N_s \cdot m$ neurons with the highest activation rates. And we construct the shared experts as follows:

$$\begin{aligned} \mathbf{W}_{up}^s &= \mathbf{W}_{up}[:, S_{N_s}]; \quad \mathbf{W}_{gate}^s = \mathbf{W}_{gate}[:, S_{N_s}]; \quad \mathbf{W}_{down}^s = \mathbf{W}_{down}[S_{N_s}, :]; \\ \implies E^s(\mathbf{x}) &= \mathbf{h}^s \mathbf{W}_{down}^s, \text{ with } \mathbf{h}^s = \text{Swish}(\mathbf{x} \mathbf{W}_{gate}^s) \odot (\mathbf{x} \mathbf{W}_{up}^s). \end{aligned} \quad (5)$$

Here, $\mathbf{W}_{up}^s \in \mathbb{R}^{d \times N_s \cdot m}$, $\mathbf{W}_{gate}^s \in \mathbb{R}^{d \times N_s \cdot m}$ and $\mathbf{W}_{down}^s \in \mathbb{R}^{N_s \cdot m \times d}$ are the weights of linear layers of the shared experts E^s . More detailed analysis is given in Appendix A.

To construct N_r **routed experts**, the key idea is to cluster the neurons that are always activated simultaneously. We first identify N_r centroids by selecting neurons (excluding those already assigned to shared experts) with the highest activation rates. We group their feature vectors into a centroid set $C = \{\mathbf{c}_i : \mu_i \in \text{TopK}(\mu_j \mid 1 \leq j \leq d_h, j \notin S_{N_s}, N_r)\} = \{\hat{\mathbf{c}}_1, \dots, \hat{\mathbf{c}}_{N_r}\}$, where $\mu = [\mu_1, \mu_2, \dots, \mu_{d_h}]$ is the activation rate averaged from the marker \mathbf{a} and we relabel the centroids as $\hat{\mathbf{c}}$. Each feature vector \mathbf{c} encapsulates the activation status of a specific neuron across the calibration dataset. We hypothesize that neurons with similar functionalities exhibit similar activation patterns—specifically, they tend to be activated and deactivated together during inference. Based on this principle, we compute the L_2 distance between each feature vector \mathbf{c} and each centroid $\hat{\mathbf{c}}$.

We formalize this by constructing a distance matrix $\mathbf{D} \in \mathbb{R}^{N_r \cdot m \times N_r}$, where element $d_{i,j}$ represents the L_2 distance between the i -th feature vector \mathbf{c}_i and the j -th centroid $\hat{\mathbf{c}}_j$:

$$d_{i,j} = \|\mathbf{c}_i - \hat{\mathbf{c}}_j\|_2 = \sqrt{\sum_{k=1}^q (c_{k,i} - \hat{c}_{k,j})^2}. \quad (6)$$

To group the neurons into routed experts, with the centroids designed above at $t = 0$, we adopt the constrained balanced K -means clustering method. Given mN_r vectors \mathbf{c} , the cluster membership value m and cluster centroids $\hat{\mathbf{c}}_1^t, \hat{\mathbf{c}}_2^t, \dots, \hat{\mathbf{c}}_{N_r}^t$ at iteration t , compute $\hat{\mathbf{c}}_1^{t+1}, \hat{\mathbf{c}}_2^{t+1}, \dots, \hat{\mathbf{c}}_{N_r}^{t+1}$ at iteration $t + 1$ with the following 2 steps:

Cluster Assignment. Let $T_{i,p}^t$ be a solution to the following linear program with $\hat{\mathbf{c}}_p^t$ fixed:

$$\begin{aligned} \min_T & \sum_{i=1}^{mN_r} \sum_{p=1}^{N_r} T_{i,p} \cdot d_{i,p} \\ \text{s.t.} & \sum_{i=1}^{mN_r} T_{i,p} = m, \forall p \in \{1, \dots, N_r\}; \quad \sum_{p=1}^{N_r} T_{i,p} = 1, \forall i \in \{1, \dots, mN_r\}; \quad T_{i,p} \geq 0, \forall p, i. \end{aligned} \quad (7)$$

Cluster Update. Update $\hat{\mathbf{c}}_p^{t+1}$ as follows:

$$\hat{\mathbf{c}}_p^{t+1} = \begin{cases} \frac{\sum_{i=1}^{mN_r} T_{i,p}^t \cdot \mathbf{c}_i}{\sum_{i=1}^{mN_r} T_{i,p}^t}, & \text{if } \sum_{i=1}^{mN_r} T_{i,p}^t > 0, \\ \hat{\mathbf{c}}_p^t, & \text{otherwise.} \end{cases} \quad (8)$$

The stopping criterion is $\hat{\mathbf{c}}_p^{t+1} = \hat{\mathbf{c}}_p^t, \forall p = 1, \dots, N_r$. We include the distance value $d_{i,j}$ into the cost function so that the balanced K -means clustering makes the intra-expert distances low and inter-expert distances high. However, the cluster assignment method defined above is an unbalanced assignment

problem ($mN_r > m$) and cannot be solved directly by existing algorithms for balanced assignment. Therefore, we reduce it to a balanced assignment by extending the distance matrix \mathbf{D} as follows:

$$\mathbf{D}^{ext} = [\underbrace{\mathbf{d}_1, \dots, \mathbf{d}_1}_{m \text{ times}}, \underbrace{\mathbf{d}_2, \dots, \mathbf{d}_2}_{m \text{ times}}, \dots, \underbrace{\mathbf{d}_{N_r}, \dots, \mathbf{d}_{N_r}}_{m \text{ times}}],$$

where we repeat every column \mathbf{d} of \mathbf{D} m -times to obtain the extended matrix $\mathbf{D}^{ext} \in \mathbb{R}^{N_r \cdot m \times N_r \cdot m}$. Then the reduced balanced assignment problem is formulated as:

Balanced Assignment. Let $T'_{i,p'}$ be a solution to the following linear program with $\hat{\mathbf{c}}_p^t$ fixed:

$$\begin{aligned} \min_{T'} & \sum_{i=1}^{mN_r} \sum_{p'=1}^{N_r \cdot m} T'_{i,p'} \cdot d_{i,p'}^{ext} \\ \text{s.t.} & \sum_{i=1}^{mN_r} T'_{i,p'} = 1, \forall p' \in \{1, \dots, mN_r\}; \sum_{p'=1}^{mN_r} T'_{i,p'} = 1, \forall i \in \{1, \dots, mN_r\}; T'_{i,p'} \geq 0, \forall i, p', \end{aligned} \quad (9)$$

where $d_{i,p'}^{ext} = d_{i,p}$ if $mp < p' \leq m(p+1)$. The **balanced cluster** $\hat{\mathbf{c}}_p^{t+1}$ can be updated as follows:

$$\hat{\mathbf{c}}_p^{t+1} = \begin{cases} \frac{\sum_{k=k_0}^{mp} \sum_{i=1}^{N_r \cdot m} T'_{i,k} \cdot \mathbf{c}_i}{\sum_{k=k_0}^{mp} \sum_{i=1}^{N_r \cdot m} T'_{i,k}}, & \text{if } \sum_{k=k_0}^{mp} \sum_{i=1}^{N_r \cdot m} T'_{i,k} > 0, \\ \hat{\mathbf{c}}_p^t, & \text{otherwise,} \end{cases} \quad (10)$$

where $k_0 = m(p-1) + 1$. The final solution T' gives us the optimized strategy to group the routed experts. We get the selection indices set $S_{N_r,p}$, $p = 1, \dots, N_r$, for each routed expert E_p^r :

$$S_{N_r,p} = \{i : \exists T'_{i,k} = 1, \text{ for } \forall k \in \{m(p-1) + 1, \dots, m\}\}.$$

We then build the weights $\mathbf{W}_{up}^{r,p} \in \mathbb{R}^{d \times m}$, $\mathbf{W}_{gate}^{r,p} \in \mathbb{R}^{d \times m}$ and $\mathbf{W}_{down}^{r,p} \in \mathbb{R}^{m \times d}$ of each routed expert E_p^r as in (5). And the output of E_p^r is given by:

$$E_p^r(\mathbf{x}) = \mathbf{h}_p^r \mathbf{W}_{down}^{r,p}, \text{ with } \mathbf{h}_p^r = \text{Swish}(\mathbf{x} \mathbf{W}_{gate}^{r,p}) \odot (\mathbf{x} \mathbf{W}_{up}^{r,p}).$$

Suppose the MoE activates N_k experts out of the N_r routed experts. We expect the router to choose the routed experts with top N_k scores. Therefore, we modify the MoE-version FFN as in (11),

$$\begin{aligned} F_{MoE}(\mathbf{x}) &= E^s(\mathbf{x}) + \sum_{i=1}^{N_r} g_i E_i^r(\mathbf{x}), \\ g_i &= \begin{cases} 1, & s_i \in \text{TopK}(\{s_i | 1 \leq j \leq N_r\}, N_k), \\ 0, & \text{otherwise,} \end{cases} \quad \text{and } \mathbf{s} = [s_1, s_2, \dots, s_{N_r}] = G(\mathbf{x}), \end{aligned} \quad (11)$$

where we make the expert score $g_i \in \{0, 1\}$ to enable an un-scaled version of the expert output to avoid biases.

3.2 Training-free Router Construction

Unlike previous works, which either built the router from scratch or intuitively used hidden features as initialization, we formulate the router construction as a minimization problem and then develop an algorithm with analysis to construct the router by approximating the optimal solution.

Given the same input embedding \mathbf{x} , the output of original output of the dense FFN is equivalent to the sum of the output of all the experts in F_{MoE} : $F(\mathbf{x}) = E^s(\mathbf{x}) + \sum_{i=1}^{N_r} E_i^r(\mathbf{x})$. The only difference roots in the expert score \mathbf{g} , which is obtained from the TopK selection of the output of G . Therefore, to preserve important knowledge captured by the original dense FNN, G can be constructed to enforce $F_{MoE}(\mathbf{x})$ to be close to $F(\mathbf{x})$ by solving the minimization problem (12),

$$\arg \min_G |F_{MoE}(\mathbf{x}; G) - F(\mathbf{x})| = \arg \min_G \left| \sum_{i=1}^{N_r} (g_i - 1) E_i^r(\mathbf{x}) \right| = \arg \min_G \left| \sum_{i \in S_{de}} E_i^r(\mathbf{x}) \right|, \quad (12)$$

where $S_{de} = \{i : s_i \notin \text{TopK}(\{s_i | 1 \leq j \leq N_r\}, N_k)\}$ and $|S_{de}| = N_r - N_k$, and the problem becomes constructing the G to minimize the absolute sum of the output of deactivated routed experts.

Note that we have made a hypothesis in (3) that the output/sparsity of $F(x)$ is highly related to the norm/sparsity of \mathbf{h} , which is the same for the expert outputs. We reformulate (12) as in (13):

$$\begin{aligned} \arg \min_G \left| \sum_{i \in S_{de}} E_i^r(\mathbf{x}) \right| &\stackrel{\text{by (2)}}{=} \arg \min_G \left| \sum_{i \in S_{de}} \sum_{j \in S_{N_r, i}} h_j \mathbf{w}_{down, j} \right| \\ &\stackrel{\text{by (3)}}{\approx} \arg \min_G \left| \sum_{i \in S_{de}} \left(\sum_{j \in S_{N_r, i}} |h_j| \right) \right| = \arg \min_G \mathbb{E}_{\mathbf{h}} [\|\mathbf{h}_i^r\|_1 \mid i \in S_{de}]. \end{aligned} \quad (13)$$

The problem becomes constructing G that can minimize the expected hidden states \mathbf{h} of deactivated routed experts. Note that G controls the de-/activation of routed experts by outputting the token-to-expert affinity $\mathbf{s} = [s_1, \dots, s_{N_r}]$. Therefore, a solution for the above problem is to construct the G such that matching the sorting indices of the set $\{s_1, \dots, s_{N_r}\}$ and the set $\{\bar{\mathbf{h}}_1^r, \dots, \bar{\mathbf{h}}_{N_r}^r\}$ ($\bar{\mathbf{h}}_i^r = \mathbb{E}_{\mathbf{h}} [\|\mathbf{h}_i^r\|_1]$), i.e. \exists permutation σ such that:

$$s_{\sigma(1)} \leq s_{\sigma(2)} \leq \dots \leq s_{\sigma(N_r)} \text{ and } \bar{\mathbf{h}}_{\sigma(1)}^r \leq \bar{\mathbf{h}}_{\sigma(2)}^r \leq \dots \leq \bar{\mathbf{h}}_{\sigma(N_r)}^r, \quad (14)$$

by which we can verify that the minimum of (13) is:

$$\min_G \mathbb{E}_{\mathbf{h}} [\|\mathbf{h}_i^r\|_1 \mid i \in S_{de}] = \frac{1}{N_r - N_k} \sum_{i=1}^{N_r - N_k} \bar{\mathbf{h}}_{\sigma(i)}^r, \quad (15)$$

which is obtained by setting $G(\mathbf{x})$ as:

$$S_{de} = \{\sigma(1), \dots, \sigma(N_r - N_k)\} = \{i : s_i \notin \text{TopK}(\{s_i | 1 \leq j \leq N_r\}, N_k)\}. \quad (16)$$

The neuron closest to the centroid in each cluster is considered as the representative neuron:

$$R_j = i, \text{ if } \|\mathbf{c}_i - \hat{\mathbf{c}}_j\|_2 \leq \|\mathbf{c}_k - \hat{\mathbf{c}}_j\|_2, \forall k \in S_{N_r, j}. \quad (17)$$

Therefore, when we regard the hidden state value $h_{R_j}^r$ as feature of the representative neuron and assume that $h_{R_j}^r \approx \bar{\mathbf{h}}_j^r$, where $\bar{\mathbf{h}}_j^r$ refers to the expected hidden state value, we can construct the router by grouping the representative neurons of all the routed experts:

$$G(\mathbf{x}) = \text{Swish}(\mathbf{x} \mathbf{W}_{gate}^R) \odot (\mathbf{x} \mathbf{W}_{up}^R), \quad (18)$$

where $\mathbf{W}_{gate}^R = \mathbf{W}_{gate}[:, S_R]$, $\mathbf{W}_{up}^R = \mathbf{W}_{up}[:, S_R]$, and $S_R = \{R_1, \dots, R_{N_r}\}$. This leads to

$$G(\mathbf{x}) = [s_1, s_2, \dots, s_{N_r}] = [h_{R_1}^r, h_{R_2}^r, \dots, h_{R_{N_r}}^r] \approx [\bar{\mathbf{h}}_1^r, \bar{\mathbf{h}}_2^r, \dots, \bar{\mathbf{h}}_{N_r}^r], \quad (19)$$

which is hence an approximate solution for the original problem introduced in (12).

3.3 Differentiable Routing and Load-balancing

Though we have constructed a well-designed router in Section 3.2, it is not differentiable since each expert score g_i is a constant, as shown in (11), hindering further alignment and performance recovery. Therefore, we introduce a learnable parameter \mathbf{u} when computing the expert scores as follows,

$$g_i = \begin{cases} 1 + s'_i \cdot u_i, & s'_i \in \text{TopK}(\{s'_i | 1 \leq j \leq N_r\}, N_k), \\ 0, & \text{otherwise,} \end{cases} \quad \mathbf{s}' = \text{Softmax}(\mathbf{s}), \text{ \& } \mathbf{u} = [u_1, u_2, \dots, u_{N_r}],$$

where the scale \mathbf{u} is initialized as zero to avoid perturbation.

For load balancing, we introduce a bias term \mathbf{b} before the TopK selection as follows:

$$g_i = \begin{cases} 1 + s'_i \cdot u_i, & s'_i + b_i \in \text{TopK}(\{s'_i | 1 \leq j \leq N_r\}, N_k), \\ 0, & \text{otherwise,} \end{cases} \quad \text{and } \mathbf{b} = [b_1, b_2, \dots, b_{N_r}].$$

Here, \mathbf{b} is initialized as zero and updated based on the expert load status during each step of training, as in DeepSeek-V3. The hyper-parameter update speed γ is used to update the bias term \mathbf{b} at the end of each step, i.e. decreasing/increasing the bias term by γ if the corresponding expert is overloaded/underloaded.

Table 1: Language modeling perplexity (PPL) on WikiText-2 and C4 validation sets. Lower is better. CMoE variants vary activation ratio (fixed 1:1 shared/routed). ‘TF’: Training-Free, ‘FT’: LoRA fine-tuned on 2k WikiText-2 samples.

Method	Act.	Llama-2 7B				Llama-3 8B			
		WikiText-2		C4		WikiText-2		C4	
		TF	FT	TF	FT	TF	FT	TF	FT
Dense	100%	5.27	-	7.27	-	6.14	-	9.44	-
LLaMA-MoE	25%	nan	468.00	nan	2660.68	nan	988.20	nan	7521.83
LLaMA-MoE-v2	25%	>10k	17.72	>10k	55.10	>60k	2754.80	>50k	5300.97
CMoE	25%	62.30	12.73	136.12	32.37	143.38	21.01	284.19	65.57
LLaMA-MoE	75%	>60k	322.20	>50k	2061.88	>500k	970.29	>400k	7079.15
LLaMA-MoE-v2	75%	>10k	8.68	7358.15	19.76	>10k	1411.23	>10k	2843.39
CMoE	75%	7.02	5.69	10.98	10.21	10.16	8.26	17.35	17.06

Table 2: Comparison of downstream tasks. Higher is better. Randomly select samples from WikiText-2 training dataset as calibration and training data.

Model	Method	Act.	FT	BoolQ(32)	SciQ	PIQA	WinoGrande(5)	ARC-C(25)	HellaSwag(10)
LLaMA-2-7B	Dense	-	-	82.04	90.80	78.78	73.95	53.15	78.55
	LLaMA-MoE	25%	✓	37.83	20.00	49.73	50.12	25.79	26.18
	LLaMA-MoE-v2	25%	✓	51.25	67.00	56.64	52.88	25.68	35.10
	CMoE	25%	✗	46.09	65.30	52.77	48.70	23.80	30.12
	CMoE	25%	✓	55.04	77.50	57.12	54.06	27.56	38.79
	LLaMA-MoE	75%	✓	37.83	20.00	49.35	50.28	26.37	25.77
	LLaMA-MoE-v2	75%	✓	49.24	79.50	63.55	59.35	34.81	54.89
	CMoE	75%	✗	71.68	88.60	73.94	65.90	41.98	69.21
	CMoE	75%	✓	75.72	89.60	74.34	67.40	43.94	70.36
	Dense	-	-	83.48	94.2	80.79	77.50	59.72	82.16
LLaMA-3-8B	LLaMA-MoE	25%	✓	37.82	20.30	49.02	50.74	25.68	25.76
	LLaMA-MoE-v2	25%	✓	48.53	45.80	50.87	48.38	24.91	27.31
	CMoE	25%	✗	47.43	47.70	52.56	50.67	23.72	28.08
	CMoE	25%	✓	56.88	72.00	57.34	51.93	25.77	36.68
	LLaMA-MoE	75%	✓	37.83	20.60	51.31	49.80	26.19	26.08
	LLaMA-MoE-v2	75%	✓	53.30	50.00	50.00	51.38	24.49	28.42
	CMoE	75%	✗	58.29	89.90	72.36	65.03	47.52	66.94
	CMoE	75%	✓	69.20	88.70	72.80	66.30	48.80	70.63

4 Experiments

CMoE is implemented using Hugging Face Transformers [27] and PyTorch [28]. We use samples from WikiText-2 [29] for calibration and initial fine-tuning, and SlimPajama [30] for extended fine-tuning experiments.

Calibration: We randomly select 8 examples (2048 sequence length) from WikiText-2 to compute activation statistics for neuron grouping and initial router construction (Eq. 20). We set $K_a = 10$ for the activation status record, which sounds counter-intuitive but works best in practice.

Lightweight Fine-tuning (2k): We fine-tune using LoRA [31] (rank 8, alpha 32) on 2,048 WikiText-2 samples for 1 epoch. The optimizer is Adam [32] ($\beta_1 = 0.9, \beta_2 = 0.95$). We use different learning rates for the router scale parameter (0.001) and other LoRA parameters (5.95e-5). The load balancing bias update speed $\gamma = 0.001$.

Extended Fine-tuning (SlimPajama): To assess performance recovery potential, we conduct further fine-tuning on subsets of the diverse SlimPajama [30] dataset (up to 1.2B tokens), using similar LoRA settings and run 1 epoch.

4.1 Main Results

We compare CMoE against several baselines on PPL, downstream task performance and inference three aspects. (1) **Dense Models:** The original Llama-2 7B and Llama-3 8B checkpoints. (2) **LLaMA-MoE [12]:** Random neuron split followed by continual pre-training (we evaluate its training-free state and after our lightweight 2k fine-tune for comparison). (3) **LLaMA-MoE-v2 [13]:** Initialize router networks based on hidden features input and do importance-based neuron partition by measuring the loss change of neuron pruned.

Our main CMoE configurations vary the activation ratio (Total Activated Experts / Total Experts) while keeping the ratio of shared-to-routed experts 1:1. For example, 25% activation uses S1A1E8 (1 shared + 1 active routed / 8 total). For baselines, we also use 8 total experts in default.

Table 3: Measured inference speedup for various CMoE activation configurations. **S**: Shared experts; **A**: Active routed experts; **E**: Total experts. E.g. S1A1E8 (1 shared + 1 active routed) / 8 total.

Configuration	Act.	Memory-Bound		Compute-Bound	
		FFN Speedup	Full Model Speedup	FFN Speedup	Full Model Speedup
S1A1E8	25%	3.6×	1.5×	3.75×	1.6×
S1A3E16	25%	3.2×	1.4×	3.45×	1.5×
S3A3E8	75%	1.25×	1.05×	1.27×	1.12×
S3A9E16	75%	1.15×	1.02×	1.09×	1.05×

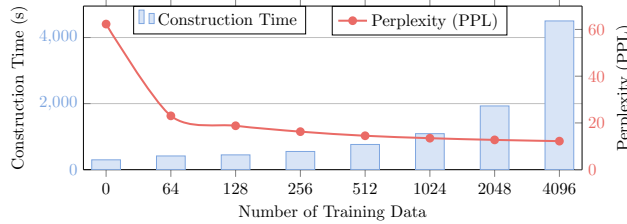


Figure 2: Trade-off between Model Performance (PPL) and Construction Time with Increasing Fine-tuning Data (WikiText-2 samples, 25% activation).

Evaluation on PPL. Table 1 presents the perplexity values for the WikiText-2 [29] and C4 [33] validation sets. In the training-free scenario, CMoE achieves approximately 60 on WikiText-2 when 25% of its components are activated, thereby showcasing its immediate practical utility, but LLaMA-MoE and LLaMA-MoE-v2 both suffer from catastrophic degradation, resulting in perplexity values greater than 20,000 or even NaN without any training. When subjected to a lightweight 2k fine-tuning process, CMoE experiences a notable reduction in perplexity across all activation ratios as expected. Specifically, 75% activation setting allows CMoE to perform on par with the dense model, evidenced by nearly PPL values. Further enhancements through extended fine-tuning is explored in the Ablation Studies section.

Evaluation on Downstream Task Performance. Table 2 presents zero-shot and few-shot results on benchmarks including: 32-shot BoolQ [34], 0-shot PIQA [35], 0-shot SciQ [36], 5-shot Winogrande [37], 25-shot ARC-Challenge [38], and 10-shot HellaSwag [39]. Similar trends emerge: CMoE is functional training-free, substantially outperforming other methods like LLaMA-MoE and LLaMA-MoE-v2 that collapse without training. Lightweight 2k fine-tuning yields significant gains; for the 25% activation CMoE, we recover $> 76\%$ of the dense model’s accuracy on SciQ and BoolQ. Increasing the activation ratio further closes the gap to the dense model. Comparisons with Dense-Small models and the impact of extended fine-tuning are detailed in the Ablation Studies (Section 4.2).

Evaluation on Inference Speedup. We measure inference latency on one single GPU. Table 3 shows speedups for the MLP layers and the full model end-to-end. Even with the overhead of routing and non-MLP layers, CMoE achieves substantial end-to-end speedups, ranging from $1.4\times$ to $1.6\times$ depending on batch size and configuration. This validates that CMoE can achieve practical efficiency enhancements, even though there is a slight performance compromise at high levels of sparsity.

4.2 Ablation Studies

We conduct ablations using Llama-2 7B and WikiText-2 data unless otherwise noted.

Impact of Fine-tuning Data Size. Figure 2 illustrates the trade-off between fine-tuning data size (using WikiText-2 samples) and construction time versus perplexity (PPL) for the CMoE 25% activation configuration. Performance improves rapidly initially when increasing data from 0 to 1,024 samples, but gains diminish significantly afterwards, while the time cost increases non-linearly. For instance, increasing samples from 2,048 to 4,096 only marginally improves PPL (12.72 to 12.21) but increases runtime by 133%. This suggests that lightweight fine-tuning (e.g., 2k samples) is highly effective, and substantial further gains likely require more diverse datasets like SlimPajama (see Section 4.2) rather than simply more of the same fine-tuning data.

Load Balancing. Figure 3 demonstrates the effectiveness of our load balancing mechanism (Section 3.3) on the final layer of Llama-2 7B, which exhibits highly skewed activation without balancing. The mechanism successfully distributes load more evenly across experts.

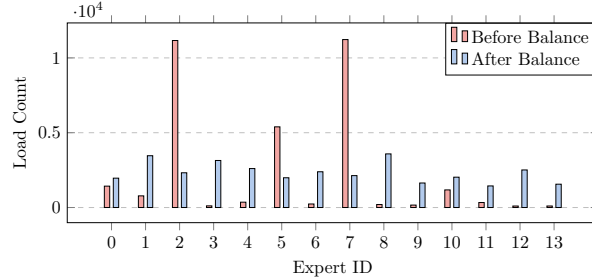


Figure 3: Effect of Load Balancing on expert utilization in Llama-2 7B final block (25% activation).

Table 4: Comparison with smaller dense models after fine-tuning on SlimPajama. CMoE uses 25% activation (S1A1E8 configuration).

Model	Training Data	PIQA	BoolQ	HellaSwag	Winogrande
Pythia-1.0B	299B	69.21	57.83	47.16	53.43
TinyLlama-1.1B	3T	73.29	57.83	59.20	59.12
CMoE-25%	training-free	52.77	46.09	28.08	50.67
CMoE-25%	2k WikiText-2	57.12	55.04	36.68	51.93
CMoE-25%	0.5B SlimPajama	59.41	57.13	41.84	53.67
CMoE-25%	1.2B SlimPajama	61.64	59.51	44.02	55.88

Table 5: Performance of different CMoE configurations at a fixed 25% activation ratio (Llama-2 7B).

Configuration	WikiText-2 ↓		C4 ↓		BoolQ ↑		SciQ ↑	
	TF	FT	TF	FT	TF	FT	TF	FT
S1A1E8	60.86	12.76	135.61	32.12	46.09	55.04	65.30	77.50
S2A2E16	62.30	12.73	136.12	32.37	53.85	57.19	66.50	77.30
S1A3E16	89.19	13.84	180.65	33.56	50.79	53.66	62.00	75.30

Comparison with Dense-Small Models and Extended Fine-tuning. Table 4 compares CMoE (25% activation) against Pythia-1.0B and TinyLlama-1.1B, which have roughly similar active parameter counts. The table also shows CMoE performance after fine-tuning on up to 1.2B tokens from the diverse SlimPajama dataset. Training-free CMoE underperforms the pre-trained dense-small models. However, after lightweight 2k fine-tuning, CMoE becomes competitive. With extended fine-tuning (1.2B tokens), CMoE surpasses Pythia-1.0B on several benchmarks and approaches TinyLlama-1.1B, despite using vastly less training data than either (1.2B vs 299B/3T tokens). This demonstrates that CMoE effectively transfers knowledge from the base model and benefits significantly from further, albeit still relatively modest, fine-tuning.

Impact of Expert Configuration (25% Activation). We compare different expert configurations while keeping the total activation ratio fixed at 25%. Table 5 shows that configurations like S1A1E8 and S2A2E16, which balance shared and routed experts, generally perform well. S1A1E8 slightly edges out S2A2E16 in PPL, potentially due to simpler routing, while S2A2E16 shows slightly better performance on BoolQ. S1A3E16, with more complex routing (3 active routed experts), shows slightly worse performance.

5 Conclusion

We present CMoE, a framework that efficiently carves sparse Mixture-of-Experts (MoE) architectures from dense LLMs through parameter reorganization and lightweight adaptation. By leveraging activation sparsity patterns in FFN layers, CMoE groups neurons into shared and routed experts via a novel balanced linear assignment formulation. The router is analytically initialized from activation statistics and refined via differentiable scaling and load balancing. Experiments demonstrate that increasing the activation ratio to 75% achieves remarkable results, delivering lossless precision from the perspective of the perplexity while still maintaining a 5% acceleration. After a brief LoRA fine-tuning process (requiring only 1 hour and 2,000 samples) successfully recovers over 76% of the dense model’s downstream accuracy, highlighting the practical efficiency of this approach for resource-constrained deployment scenarios, which outperforms the baselines LLaMA-MoE and LLaMA-MoE-v2. Extensive experiments have demonstrated that CMoE offers a practical approach for deploying large language models (LLMs) in resource-constrained environments.

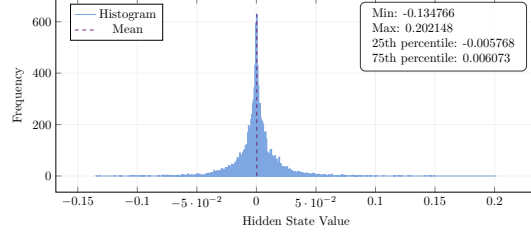
References

- [1] Susan Zhang, Stephen Roller, Naman Goyal, Mikel Artetxe, Moya Chen, Shuohui Chen, Christopher Dewan, Mona Diab, Xian Li, Xi Victoria Lin, et al. Opt: Open pre-trained transformer language models. *arXiv preprint arXiv:2205.01068*, 2022.
- [2] Hugo Touvron, Louis Martin, Kevin Stone, Peter Albert, Amjad Almahairi, Yasmine Babaei, Nikolay Bashlykov, Soumya Batra, Prajjwal Bhargava, Shruti Bhosale, et al. Llama 2: Open foundation and fine-tuned chat models. *arXiv preprint arXiv:2307.09288*, 2023.
- [3] Haotian Liu, Chunyuan Li, Qingyang Wu, and Yong Jae Lee. Visual instruction tuning. *Advances in neural information processing systems*, 36, 2024.
- [4] Aixiu Liu, Bei Feng, Bing Xue, Bingxuan Wang, Bochao Wu, Chengda Lu, Chenggang Zhao, Chengqi Deng, Chenyu Zhang, Chong Ruan, et al. Deepseek-v3 technical report. *arXiv preprint arXiv:2412.19437*, 2024.
- [5] Dmitry Lepikhin, HyukJoong Lee, Yuanzhong Xu, Dehao Chen, Orhan Firat, Yanping Huang, Maxim Krikun, Noam Shazeer, and Zhifeng Chen. Gshard: Scaling giant models with conditional computation and automatic sharding. *arXiv preprint arXiv:2006.16668*, 2020.
- [6] Nan Du, Yanping Huang, Andrew M Dai, Simon Tong, Dmitry Lepikhin, Yuanzhong Xu, Maxim Krikun, Yanqi Zhou, Adams Wei Yu, Orhan Firat, et al. Glam: Efficient scaling of language models with mixture-of-experts. In *International Conference on Machine Learning*, pages 5547–5569. PMLR, 2022.
- [7] William Fedus, Barret Zoph, and Noam Shazeer. Switch transformers: Scaling to trillion parameter models with simple and efficient sparsity. *Journal of Machine Learning Research*, 23(120):1–39, 2022.
- [8] Damai Dai, Chengqi Deng, Chenggang Zhao, RX Xu, Huazuo Gao, Deli Chen, Jiashi Li, Wangding Zeng, Xingkai Yu, Y Wu, et al. Deepseekmoe: Towards ultimate expert specialization in mixture-of-experts language models. *arXiv preprint arXiv:2401.06066*, 2024.
- [9] Zichang Liu, Jue Wang, Tri Dao, Tianyi Zhou, Binhang Yuan, Zhao Song, Anshumali Shrivastava, Ce Zhang, Yuandong Tian, Christopher Re, et al. Deja vu: Contextual sparsity for efficient llms at inference time. In *International Conference on Machine Learning*, pages 22137–22176. PMLR, 2023.
- [10] Zhengyan Zhang, Yankai Lin, Zhiyuan Liu, Peng Li, Maosong Sun, and Jie Zhou. Moefication: Transformer feed-forward layers are mixtures of experts. *arXiv preprint arXiv:2110.01786*, 2021.
- [11] Zehua Pei, Hui-Ling Zhen, Xianzhi Yu, Sinno Jialin Pan, Mingxuan Yuan, and Bei Yu. Fusegpt: Learnable layers fusion of generative pre-trained transformers. *arXiv preprint arXiv:2411.14507*, 2024.
- [12] Tong Zhu, Xiaoye Qu, Daize Dong, Jiacheng Ruan, Jingqi Tong, Conghui He, and Yu Cheng. Llama-moe: Building mixture-of-experts from llama with continual pre-training. In *Proceedings of the 2024 Conference on Empirical Methods in Natural Language Processing*, pages 15913–15923, 2024.
- [13] Xiaoye Qu, Daize Dong, Xuyang Hu, Tong Zhu, Weigao Sun, and Yu Cheng. Llama-moe v2: Exploring sparsity of llama from perspective of mixture-of-experts with post-training. *arXiv preprint arXiv:2411.15708*, 2024.
- [14] Haizhong Zheng, Xiaoyan Bai, Xueshen Liu, Z Morley Mao, Beidi Chen, Fan Lai, and Atul Prakash. Learn to be efficient: Build structured sparsity in large language models. *arXiv preprint arXiv:2402.06126*, 2024.
- [15] Roy Jonker and Ton Volgenant. A shortest augmenting path algorithm for dense and sparse linear assignment problems. In *DGOR/NSOR: Papers of the 16th Annual Meeting of DGOR in Cooperation with NSOR/Vorträge der 16. Jahrestagung der DGOR zusammen mit der NSOR*, pages 622–622. Springer, 1988.
- [16] Simiao Zuo, Qingru Zhang, Chen Liang, Pengcheng He, Tuo Zhao, and Weizhu Chen. Moe-bert: from bert to mixture-of-experts via importance-guided adaptation. *arXiv preprint arXiv:2204.07675*, 2022.
- [17] Yuanhang Yang, Shiyi Qi, Wenchao Gu, Chaozheng Wang, Cuiyun Gao, and Zenglin Xu. Xmoe: Sparse models with fine-grained and adaptive expert selection. *arXiv preprint arXiv:2403.18926*, 2024.

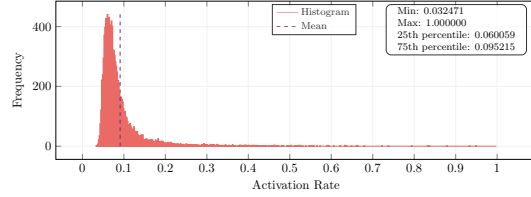
- [18] Aran Komatsuzaki, Joan Puigcerver, James Lee-Thorp, Carlos Riquelme Ruiz, Basil Mustafa, Joshua Ainslie, Yi Tay, Mostafa Dehghani, and Neil Houlsby. Sparse upcycling: Training mixture-of-experts from dense checkpoints. *arXiv preprint arXiv:2212.05055*, 2022.
- [19] Haoyuan Wu, Haisheng Zheng, Zhuolun He, and Bei Yu. Parameter-efficient sparsity crafting from dense to mixture-of-experts for instruction tuning on general tasks. *arXiv preprint arXiv:2401.02731*, 2024.
- [20] Ji Lin, Jiaming Tang, Haotian Tang, Shang Yang, Wei-Ming Chen, Wei-Chen Wang, Guangxuan Xiao, Xingyu Dang, Chuang Gan, and Song Han. Awq: Activation-aware weight quantization for on-device llm compression and acceleration. *Proceedings of Machine Learning and Systems*, 6:87–100, 2024.
- [21] Zehua Pei, Xufeng Yao, Wenqian Zhao, and Bei Yu. Quantization via distillation and contrastive learning. *IEEE Transactions on Neural Networks and Learning Systems*, 2023.
- [22] Lancheng Zou, Wenqian Zhao, Shuo Yin, Chen Bai, Qi Sun, and Bei Yu. Bie: Bi-exponent block floating-point for large language models quantization. In *Forty-first International Conference on Machine Learning*, 2024.
- [23] Yujun Lin, Haotian Tang, Shang Yang, Zhekai Zhang, Guangxuan Xiao, Chuang Gan, and Song Han. Qserve: W4a8kv4 quantization and system co-design for efficient llm serving. *arXiv preprint arXiv:2405.04532*, 2024.
- [24] Xudong Lu, Qi Liu, Yuhui Xu, Aojun Zhou, Siyuan Huang, Bo Zhang, Junchi Yan, and Hongsheng Li. Not all experts are equal: Efficient expert pruning and skipping for mixture-of-experts large language models. *arXiv preprint arXiv:2402.14800*, 2024.
- [25] Xin Men, Mingyu Xu, Qingyu Zhang, Bingning Wang, Hongyu Lin, Yaojie Lu, Xianpei Han, and Weipeng Chen. Shortgpt: Layers in large language models are more redundant than you expect. *arXiv preprint arXiv:2403.03853*, 2024.
- [26] Saleh Ashkboos, Maximilian L Croci, Marcelo Gennari do Nascimento, Torsten Hoefer, and James Hensman. SliceGPT: Compress large language models by deleting rows and columns. *arXiv preprint arXiv:2401.15024*, 2024.
- [27] T Wolf. Huggingface’s transformers: State-of-the-art natural language processing. *arXiv preprint arXiv:1910.03771*, 2019.
- [28] Adam Paszke, Sam Gross, Francisco Massa, Adam Lerer, James Bradbury, Gregory Chanan, Trevor Killeen, Zeming Lin, Natalia Gimelshein, Luca Antiga, et al. Pytorch: An imperative style, high-performance deep learning library. *Advances in neural information processing systems*, 32, 2019.
- [29] Stephen Merity, Caiming Xiong, James Bradbury, and Richard Socher. Pointer sentinel mixture models. *arXiv preprint arXiv:1609.07843*, 2016.
- [30] Daria Soboleva, Faisal Al-Khateeb, Robert Myers, Jacob R Steeves, Joel Hestness, and Nolan Dey. SlimPajama: A 627B token cleaned and deduplicated version of RedPajama. <https://cerebras.ai/blog/slimpajama-a-627b-token-cleaned-and-deduplicated-version-of-redpajama>, 2023.
- [31] Edward J Hu, Yelong Shen, Phillip Wallis, Zeyuan Allen-Zhu, Yanzhi Li, Shean Wang, Lu Wang, and Weizhu Chen. Lora: Low-rank adaptation of large language models. *arXiv preprint arXiv:2106.09685*, 2021.
- [32] Diederik P Kingma. Adam: A method for stochastic optimization. *arXiv preprint arXiv:1412.6980*, 2014.
- [33] Colin Raffel, Noam Shazeer, Adam Roberts, Katherine Lee, Sharan Narang, Michael Matena, Yanqi Zhou, Wei Li, and Peter J Liu. Exploring the limits of transfer learning with a unified text-to-text transformer. *Journal of machine learning research*, 21(140):1–67, 2020.
- [34] Christopher Clark, Kenton Lee, Ming-Wei Chang, Tom Kwiatkowski, Michael Collins, and Kristina Toutanova. Boolq: Exploring the surprising difficulty of natural yes/no questions. *arXiv preprint arXiv:1905.10044*, 2019.
- [35] Yonatan Bisk, Rowan Zellers, Jianfeng Gao, Yejin Choi, et al. Piqa: Reasoning about physical commonsense in natural language. In *Proceedings of the AAAI conference on artificial intelligence*, volume 34, pages 7432–7439, 2020.

- [36] Johannes Welbl, Nelson F Liu, and Matt Gardner. Crowdsourcing multiple choice science questions. *arXiv preprint arXiv:1707.06209*, 2017.
- [37] Keisuke Sakaguchi, Ronan Le Bras, Chandra Bhagavatula, and Yejin Choi. Winogrande: An adversarial winograd schema challenge at scale. *Communications of the ACM*, 64(9):99–106, 2021.
- [38] Peter Clark, Isaac Cowhey, Oren Etzioni, Tushar Khot, Ashish Sabharwal, Carissa Schoenick, and Oyvind Tafjord. Think you have solved question answering? try arc, the ai2 reasoning challenge. *arXiv preprint arXiv:1803.05457*, 2018.
- [39] Rowan Zellers, Ari Holtzman, Yonatan Bisk, Ali Farhadi, and Yejin Choi. Hellaswag: Can a machine really finish your sentence? *arXiv preprint arXiv:1905.07830*, 2019.

A Algorithmic Analysis



(a) The histogram of FFN hidden state \mathbf{h} for the 3-th block and the 1,000-th token.



(b) The histogram of activation rates μ for the 3-th block with $K_a = 1,000$.

Figure A.1: The proposed framework, CMoE, and the numerical analysis on its effectiveness.

As demonstrated in Figure 1(a), the distribution of the FFN hidden state \mathbf{h} is sharply peaked at 0 and constrained within a small range. This indicates that most h_i are concentrated near zero, confirming the sparsity of activations. The symmetry of the distribution suggests a near-normal distribution centered around the mean. These observations of high differentiation and independence across different neurons suggest that hidden state values serve as a robust basis for judging neuron activation, motivating the Absolute Top-K (ATopK) metric defined in Equation (4).

To quantify neuron activation patterns, we first collect activation markers from a calibration dataset. Given a batched input tensor $\mathbf{X} \in \mathbb{R}^{b \times s \times d}$, with b the batch size and s the sequence length, we obtain the batched hidden state $\mathbf{H} \in \mathbb{R}^{b \times s \times d_h}$ as follows:

$$\mathbf{H} = \text{Swish}(\mathbf{X}\mathbf{W}_{gate}) \odot (\mathbf{X}\mathbf{W}_{up}). \quad (20)$$

Note that in practical implementation, we normalize \mathbf{X} , \mathbf{W}_{gate} and \mathbf{W}_{up} before the calculation to eliminate the influence of their magnitudes on the output. Using the ATopK metric (defined in the main text), we then calculate the activation markers for the hidden state of all the tokens. These markers are reshaped into an activation feature matrix $\mathbf{A} \in \mathbb{R}^{q \times d_h}$, where $q = b \cdot s$. Denote the i -th column of \mathbf{A} as the feature vector $\mathbf{c}_i \in \mathbb{R}^q$, i.e., $\mathbf{A} = [\mathbf{c}_1 \ \mathbf{c}_2 \ \cdots \ \mathbf{c}_{d_h}]$, which represents the i -th neuron's activation status on the sampled q tokens. By calculating the expected value of each \mathbf{c}_i , we can obtain the vector of activated rates μ as:

$$\mu = [\mu_1, \mu_2, \dots, \mu_{d_h}], \text{ with } \mu_i = \frac{1}{q} \sum_{j=1}^q c_{j,i}, \quad (21)$$

where $c_{j,i}$ indicates the j -th element of \mathbf{c}_i . The histogram of these activation rates μ is shown in Figure 1(b). The histogram reveals a highly skewed distribution of activation rates, where the majority of neurons exhibit low activation rates (below 0.1), with a sharp peak near 0.07. However, the distribution also features a long tail, indicating the presence of a subset of neurons with significantly higher activation rates extending up to 1. These high-activation neurons are likely active across a wide range of input tokens, making them suitable for processing common knowledge rather than task-specific specialization. Therefore, we identify neurons for shared experts by grouping these high-activation neurons. Given the total number of shared experts as N_s and the expert size m , we get the selection indices set S_{N_s} by selecting $N_s \cdot m$ neurons with highest activation rates based on μ :

$$S_{N_s} = \{i : \mu_i \in \text{TopK}(\{\mu_j \mid 1 \leq j \leq d_h\}, N_s \cdot m)\}. \quad (22)$$

These indices S_{N_s} are then used to form the shared experts by assigning the corresponding parameters from the original FFN, as detailed in Section 3.1 (see Equation 5 in the main text).

The majority of low activation rates also encourage us to construct routed experts, which are not always activated but are specialized for tokens encountered.

B Impact of Calibration Data Size

We vary the number of calibration samples (WikiText-2) used for neuron analysis. Table B.1 shows that performance improves modestly with more calibration data, with diminishing returns beyond 32 or 64 samples. Using 8 samples provides a good balance of efficiency and effectiveness.

Table B.1: Impact of calibration data size on PPL (Llama-2 7B, CMoE 25% activation, training-free).

Calibration Samples	WikiText-2 PPL	C4 PPL
8	60.86	135.61
32	58.71	129.62
64	55.88	125.02

C Scaling to Larger Models

To verify that CMoE scales to larger models, we applied the same conversion process (using 25% activation, S1A1E8 configuration) to Llama-2 13B. Table C.1 shows the training-free PPL results using different calibration datasets. We observe similar patterns to the 7B model: performance improves with more calibration data, and using domain-matched calibration data (C4 for C4 PPL) yields better results. This confirms the applicability of CMoE to larger base models.

Table C.1: CMoE (25% activation, training-free) performance on Llama-2 13B with varying calibration data.

Calibration Data	WikiText-2 PPL	C4 PPL
8 from WikiText-2	68.82	193.66
32 from WikiText-2	56.25	167.25
32 from C4	116.77	134.93
32 WikiText-2 + 32 C4	68.59	140.17

D Discussion

Limitations While CMoE demonstrates promising results in transforming dense LLMs into efficient sparse MoE architectures, certain aspects merit consideration for future exploration. Firstly, the performance of neuron activation profiling and subsequent expert grouping is influenced by the choice of the calibration dataset. Optimal results are best achieved when the calibration data aligns well with the characteristics of the target domain or downstream tasks. Secondly, while the training-free router construction provides notable computational efficiency, it may not fully capture all nuances of routing decisions in the same way a router trained extensively end-to-end with the experts might. In some scenarios, particularly those requiring highly dynamic expert selection, there might be opportunities for further performance gains through additional fine-tuning. Future work could also explore the application and adaptation of CMoE across a wider array of model architectures and a more diverse set of downstream tasks to further understand its broader applicability and potential refinements.

Impact Statement This paper aims to contribute to the advancement of the Machine Learning field. While our work may have various societal implications, we do not find it necessary to emphasize any particular consequences here.